Alteration of cell cycle progression by Sindbis virus infection

（シンドビスウイルスが細胞周期に及ぼす影響に関する検討）

千葉大学大学院医学薬学府

先端医学薬学専攻

（主任：白澤　浩教授）

YI RUIRONG

ABSTRACT

We examined the impact of Sindbis virus (SIN) infection on cell cycle progression in a cancer cell line, HeLa, and a non-cancerous cell line, Vero. Cell cycle analyses showed that SIN infection is able to alter the cell cycle progression in both HeLa and Vero cells, but differently, especially during the early stage of infection. SIN infection affected the expression of several cell cycle regulators (CDK4, CDK6, cyclin E, p21, cyclin A and cyclin B) in HeLa cells and caused HeLa cells to accumulate in S phase during the early stage of infection. Monitoring SIN replication in HeLa and Vero cells expressing cell cycle indicators revealed that SIN which infected HeLa cells during G_1 phase preferred to proliferate during S/G_2 phase, and the average time interval for viral replication was significantly shorter in both HeLa and Vero cells infected during G_1 phase than in cells infected during S/G_2 phase. The expression of p53 was affected at the later stage of infection, and p53 expression may be involved in the efficient replication of SIN. The alteration of cell cycle progression that SIN infection causes might have an implication regarding the oncolytic feature of SIN.

Introduction

Sindbis virus (SIN) is an RNA virus belonging to the *Alphavirus* genus in the *Togaviridae* virus family. SIN is transmitted to birds and mammals by mosquito bites and subsequently spreads throughout the body through the bloodstream (Griffin, 2001). SIN infection induces no or only mild symptoms (fever, rash, and arthralgia) in humans (Jan and Griffin, 1999). SIN has the potential to induce apoptosis in infected mammalian cells, but establishes a non-cytolytic persistent infection in arthropod cells (Jan and Griffin, 1999; Moriishi et al., 2002). In addition, the 67-kDa, high-affinity laminin receptor has been identified as a surface attachment factor that mediates SIN infection of mammalian cells (Wang et al., 1992), and is highly expressed in various human cancers (van den Brûle et al., 1996; al-Saleh et al., 1997).

We reported previously that SIN has oncolytic features and demonstrates antitumoral effects in various cancers, including cervical and ovarian cancer (Unno et al., 2005), and human oral squamous carcinoma cells (Saito et al., 2009b). Replication-defective SIN vectors have also been developed to target and eradicate tumors (Tseng et al., 2002; Yamanaka, 2004). To increase anti-tumor potency, SIN vectors expressing foreign genes, such as cytokines like IL-12 (Tseng et al., 2004) and the herpes simplex virus type-1 thymidine kinase (TK) gene (Tseng et al., 2006, 2009), have been explored.

As an oncolytic virus, the favorable features of SIN include rapid production of high-titer virus, efficient infection of a variety of cancer cells, and a high RNA replication rate in the cytoplasm (Saito et al., 2009a). The preferable characteristics of

SIN for cancer therapy might be attributed to the combination of favorable viral growth and the uncontrolled cell proliferation of cancer cells, including deregulation of the cell cycle. In normal cells, cell cycle regulator proteins, cyclin-dependent protein kinases (CDKs), cyclins, and CDK inhibitory proteins regulate progression through G_1, S, G_2 and M phases in the cell cycle. Controls by these regulators are often disturbed in cancer cells, which tend to remain in cycle (Sherr, 1996). Many viruses can affect the cell cycle progression of host cells to favor viral replication. Regarding DNA viruses, such as simian virus 40, adenovirus, and papillomavirus, infected cells are promoted into S phase (reviewed by Op De Beeck and Caillet-Fauquet, 1997). Several RNA viruses also reportedly affect the cell cycle (reviewed by Emmett et al., 2005). Measles virus infection results in a G_0 block (Naniche et al., 1999), and the paramyxovirus simian virus V protein is known to prolong the cell cycle by delaying the G_1/S transition and suppressing progression through S phase (Lin and Lamb, 2000). Recently, malignant glioma cells infected with an RNA virus, alphavirus M1, were shown to accumulate in S phase by down-regulating p21 protein (Hu et al., 2009). The interaction between SIN replication and the host cell cycle has not been studied in detail, particularly in the context of oncolysis.

In this study, we analyzed the dynamics of cell cycle phases of HeLa and Vero cells infected with SIN in order to elucidate the interaction between SIN replication and the host cell cycle. SIN infection resulted in several significant alterations of cell cycle progression that differed between HeLa cells and Vero cells. Further analysis of cell cycle regulators indicated that SIN infection affected the expression of key cell

cycle regulators in HeLa cells. Experiments with cells expressing the cell cycle indicators fluorescent ubiquitination-based cell cycle indicator (Fucci)-orange and Fucci-green and SIN expressing blue fluorescence protein (BFP) revealed that SIN which infected HeLa cells during G_1 preferred to replicate during S/G_2 phase. For both HeLa and Vero cell lines, the average interval for viral replication was shorter in cells infected during G_1 than in cells infected during S/G_2. In this study, SIN infection was able to alter the cell cycle progression of infected cancer cells and exhibited a preference for the timing of viral replication among the cell cycle phases.

Materials and Methods

Cell lines

HeLa cells were obtained from the American Type Culture Collection (ATCC; Rockvile, MD). HSC-4 cells were derived from the Human Science Research Resources Bank (Osaka, Japan). Vero cells and human fibroblast cells were laboratory stock. Cells were grown in Dulbecco's modified Eagle's medium (DMEM; Sigma) with 10% fetal bovine serum (FBS) at 37ºC in 5% CO_2.

Viral stocks and construction of recombinant virus

We used the laboratory stock of the AR339 strain of SIN. The plasmid pTR339-GFP-2A was kindly provided by Dr. Hans W. Heidner (University of Texas, San Antonio, TX; Thomas et al., 2003). To substitute the BFP gene for the GFP gene in the pTR339-GFP-2A plasmid, 2.5 kbp of PCR product containing GFP-2A was amplified from pTR339-GFP-2A and ligated into the pCR2.1-Topo vector (Invitrogen). Insertion of the fragment was confirmed by sequencing. Next, the fragment was re-cloned into the pGEM-3Z vector between the *Eco*RI (5') and *Bam*HI (3') restriction sites. Then, reverse PCR without the GFP gene was performed using KOD-plus enzyme (Toyobo Life Science Department) to generate the pGEM-2A fragment. Meanwhile, the BFP gene was amplified using PCR and the KOD-plus enzyme, with primers containing 15-bp extensions homologous to the pGEM-2A fragment ends. The pGEM-2A and BFP fragments were ligated using the In-fusion HD Cloning Kit (Clontech) to yield pGEM-BFP-2A. A 2460-bp fragment containing a part of nsp4 and the full capsid was ligated into pGEM-BFP-2A between the *Eco*RI

(5') and *Nru*I (3') restriction sites to generate pGEM-C-BFP-2A. Next, pTR339-GFP-2A was digested with *Hpa*I (5') and *Bss*HII (3') restriction enzymes, and GFP was replaced with BFP from pGEM-C-BFP-2A to yield pTR339-BFP-2A.

RNA transcription and transfection

For in vitro transcription, pTR339-BFP-2A plasmid was purified using the HiSpeed Plasmid Midi Kit (Qiagen), linearized with *Xho*I (Biolab), and transcribed in vitro with the RiboMAX^{TM} Large-Scale RNA production system-SP6 kit (Promega). We used 2 μL of the transcription product per 2 μL lipofectamine^{TM} 2000 to transfect Vero cells. Three days after transfection, the virus generated from the pTR339-BFP-2A, TR339-BFP-2A, was collected and frozen at -80ºC. TR339-BFP-2A was propagated in Vero cells maintained in DMEM with 10% FBS at 37ºC in 5% CO_2. Viral titers were determined by plaque assays using monolayers of Vero cells.

Generation of HeLa and Vero cells that express Fucci-G_1 orange and Fucci-S/G_2/M green

To obtain HeLa and Vero cells that stably express Fucci-G_1 orange and Fucci-S/G_2/M green, we successively introduced two plasmids, pFucci-G_1 orange and pFucci-S/G_2/M Green-hyg (Amalgaam), into HeLa cells and Vero cells. After being pre-cultured in 6-well dishes, HeLa and Vero cells were transfected with 5 μg of pFucci-G_1 orange per 2 μL of lipofectamine 2000^{TM}. After overnight incubation of transfected cells, the cells were passaged from 6-well dishes to 10-cm dishes. To obtain stable transformants, the transfected Vero and HeLa cells were selected in medium containing 600 μg/mL and 400 μg/mL Geneticin (G418) (Invitrogen),

respectively. After 7 to 10 days of selection, the colonies that exhibited orange fluorescence in the nuclei were picked up and cultured in medium containing 200 μg/mL G418 for further selection. The HeLa and Vero cells that stably expressed Fucci orange were obtained from the selected colonies. Then, the HeLa and Vero cells that stably expressed Fucci-G_1 orange were transfected with pFucci-S/G_2/M Green-hyg. The transfected Vero and HeLa cells were selected in 250 μg/mL and 200 μg/mL hygromycin B (Wako), respectively. The colonies that exhibited both orange and green nuclei were picked up and cultured to obtain stably transformed HeLa-Fucci and Vero-Fucci cell lines.

Imaging of cultured cells

Cells were grown on a 35-mm dish in DMEM with 10% FBS. TR339-BFP-2A virus was adsorbed with cells for 30 min at 5 MOI for HeLa-Fucci cells and 1 MOI for Vero-Fucci cells. After incubation at 37ºC in 5% CO_2 for 1.5 hours, cells were subjected to long-term, time-lapse imaging using a computer-assisted fluorescence microscope (Olympus, FV10i) at 37ºC in 5% CO_2. Images were recorded every 30 min. Three filter cubes were chosen for fluorescence imaging: mKusabira-orange (excitation wavelength 548 nm, emission wavelength 559 nm) to observe Fucci orange, Azami Green (excitation wavelength 493 nm, emission wavelength 505 nm) to observe Fucci green, and Blue-Narrow (excitation wavelength at 405 nm, emission wavelength 420 - 460 nm) to observe BFP. We used Fluoview version 3.1 (Olympus) for image acquisition and analysis.

Western blotting

Cells were collected and washed twice with PBS, and an equal number of infected and mock-infected cells were resuspended in an equal volume of M-PER@ Mammalian Protein Extraction Reagent (Thermo) with a cocktail of protease inhibitor (Sigma-Aldrich) and mixed gently for 10 minutes. Lysates were centrifuged at 14,000 × *g* for 15 min. Equal volumes of extracted protein were loaded onto SDS-polyacrylamide gels (Atto Corporation), transferred onto PVDF membranes (Trans-Blot Turbo™ Transfer Pack, BIO-RAD), and analyzed with antibodies. Rabbit anti-CDK2, rabbit anti-pCDK2 (Thr 160), rabbit anti-cyclin B1, rabbit anti-p21Waf1/Cip1, mouse anti-CDK4, mouse anti-CDK6, rabbit anti-p-cdc2 (Y15), mouse anti-cyclin D1, rabbit anti-RARP, and rabbit anti-cleaved caspase-3 were obtained from Cell Signaling Technology. Rabbit anti-cyclin A, mouse anti-cyclin E, mouse anti-Cdc25A, and rabbit anti-p53 were obtained from Santa Cruz Biotechnology. Rabbit anti-β-actin and rabbit anti-caspase-3 were purchased from Abcom. Rabbit anti-capsid was prepared in our laboratory (Unno et al., 2005).

Cell cycle analysis

Cells were collected and washed twice with PBS. Next, cells were treated with reagents from the CycleTEST™ PLUS DNA Reagent Kit (Becton Dickinson and Company) and analyzed on a BD Accuri™ C6 Flow Cytometer (Becton Dickinson and Company) equipped with FACScan's fluorescence 2 (FL2) detector. The collected data was analyzed using FlowJo 7.6.5 (TreeStar Company).

Statistical analysis

All values were expressed as mean ± SD. The Mann-Whitney U-test was used to compare the time of BFP fluorescence appearance and the interval between BFP appearance and apoptosis. Significant differences between expected frequencies and observed frequencies were tested using the chi-square test. Statistical analyses were performed using the software Statcel2, version 2 (OMS, Tokyo, Japan). Values of $P < 0.05$ were considered statistically significant.

Results

Effects of SIN infection on cell cycle progression in HeLa and Vero cells

Many viruses can affect the cell cycle progression of host cells in favor of viral replication (Emmett et al., 2005). The interactions between SIN replication and host cell cycle have not been studied in detail, particularly in the context of oncolysis. To investigate the impact of SIN infection on cell cycle progression, we used fluorescence-activated cell sorting (FACS) analysis to assess the effect of SIN infection on the distribution of HeLa and Vero cells in each phase of the cell cycle. Cells infected with 1 MOI of SIN or mock-infected were subjected to FACS analysis at 2, 4, 7, and 15 hours post-infection (hpi) in HeLa cells and at 2, 4, 7, and 14 hpi in Vero cells. SIN infection significantly altered the cell cycle profile in HeLa cells (primary data are shown in Fig. 1A, and the time course of the proportion of cells in G_0/G_1, S, and G_2/M phases are shown in Fig. 1B). The proportion of HeLa cells in S phase increased and proportions of HeLa cells in G_0/G_1 and G_2/M decreased by 4 hpi, suggesting that SIN infection might simultaneously promote cell entry into S phase and prevent exit from S phase (Fig. 1A). The proportions of SIN-infected cells in each stage of the cell cycle approached the respective proportions of mock-infected cells by 7 hpi (Fig. 1B). Then, the proportions of infected cells in G_0/G_1 and S phases increased and decreased, respectively, suggesting that cell cycle progression from G_1 to S phase was blocked and that cells accumulated in G_0/G_1 at the later stage of infection.

In contrast, SIN infection caused little effect on the cell cycle progression of Vero cells during the early stage of infection (Fig. 1C). However, at the later stage of infection (by 14 hpi), the proportion of infected cells in S phase had increased and the proportions of infected cells in G_0/G_1 and G_2/M had decreased (Fig. 1D).

Effects of SIN infection on the expression of cell cycle regulators in HeLa cells

FACS analysis demonstrated that SIN infection affected cell cycle progression in both HeLa and Vero cells, but differently. To characterize the molecular basis for the effects of SIN infection on the cell cycle in HeLa cells, we examined the levels of key cell cycle regulatory proteins. These cellular proteins were collected from mock- and SIN-infected HeLa cells at 2, 4, 7, and 15 hpi, and protein levels were measured using Western blotting (Fig. 2).

Because the cyclin D/CDK4 (CDK6) complex is active during early G_1 and regulates the progression of G_1, we examined the expression of these proteins and their regulators in infected HeLa cells. Although cyclin D1 expression was not affected by SIN infection by 7 hpi, cyclin-dependent kinases CDK4 and CDK6 were both expressed at higher levels in SIN-infected cells at 4 and 7 hpi (Fig. 2A). The elevated expression of CDK4 and CDK6 may account for the acceleration of G_1 progression, followed by the decreased proportion of G_0/G_1 cells observed by FACS analysis in HeLa cells at 4 hpi.

During late G_1, the activated cyclin E/CDK2 complex promotes the G_1/S transition by phosphorylating pRB (Pestell et al., 1999). Cyclin E, the overexpression of which shortens the duration of G_1 phase independently of pRB (Resnitzky et al., 1994;

Ohtsubo et al., 1995; Lukas et al., 1997), increased significantly at 4 and 7 hpi in SIN-infected HeLa cells (Fig. 2B). The expression pattern of cyclin E in SIN-infected cells was similar to the expression patterns of CDK4 and CDK6. Total CDK2 expression in SIN-infected cells was not affected by the infection (Fig. 2B). Because CDK2 activity is regulated by phosphorylation at Thr160 and activated by Cdc25A-mediated dephosphorylation of Thr14 and Tyr15 (Gu et al., 1992), we examined the expression of p-CDK2 (Thr160) and Cdc25A. Although p-CDK2 (Thr160) levels were not affected by 7 hpi, Cdc25A was expressed at a higher level in SIN-infected cells at 7 hpi (Fig. 2B). Meanwhile, the expression of p21, which binds to and inhibits the cyclin E/CDK2 complex (Chen et al., 1995; Goubin and Ducommun, 1995), was decreased significantly in SIN-infected cells at 4 hpi (Fig. 2B). Taken together, the up-regulation of cyclin E and Cdc25A and down-regulation of p21 were thought to shorten G_1 and promote the G_1/S transition, in cooperation with CDK4/6-promoted G_1 progression. The alterations of cyclin E, Cdc25A, and p21 expression by SIN infection were considered consistent with the decrease of cells in G_1 phase and the increase of cells in S phase observed by FACS analysis.

To determine whether the decreased p21 expression at 4 hpi and the increased Cdc25A expression at 7 hpi in SIN-infected cells were the result of transcriptional regulation by p53 (Demidova et al., 2009; Shen and Huang, 2012), we measured the expression of p53. By 4 hpi, p53 expression was not affected by SIN infection, suggesting that the decrease of p21 at 4 hpi might be independent of p53 expression (Fig. 2B). On the other hand, the down-regulation of p53 expression at 7 hpi in SIN-

infected cells was considered consistent with the increase of Cdc25A at 7 hpi, because p53 inhibits Cdc25A transcription through the activation of ATF3 (Demidova et al., 2009).

Cyclin A associates with CDK2 and regulates the progression of S phase (Woo and Poon, 2003). We observed suppressed cyclin A expression in SIN-infected cells at 4 hpi (Fig. 2C). This might cause retardation of S phase, and was consistent with the decrease of cells in G_2/M phase and the increase of cells in S phase in SIN-infected HeLa cells observed by FACS analysis.

Entry into M phase is signaled by the accumulation of cyclin B-cdc2, and the activation of cdc2 requires dephosphorylation at Tyr15 and Thr14 (Dunphy 1994). Therefore, we measured the levels of cyclin B1 and phosphorylated p-cdc2 (Tyr 15) protein in SIN-infected HeLa cells. Cyclin B1 expression was suppressed in SIN-infected cells (Fig. 2C), indicating that SIN infection might block the cell cycle transition through the G_2/M checkpoint. Failure to pass the DNA replication checkpoint results in the inhibition of cdc25C activity, in turn leading to inhibition of the dephosphorylation of cdc2 (Zeng et al., 1998). Therefore, higher levels of p-cdc2 protein (the inactive form of the protein) in SIN-infected cells at 4 hpi (Fig. 2C) agreed with the temporal accumulation of cells in S phase at 4 hpi observed by FACS analysis.

At 15 hpi, the expression of cyclin D1 in infected cells was undetectable, and both CDK4 and CDK6 were expressed at low levels (Fig. 2A). The suppression of cyclin D1, CDK4, and CDK6 at 15 hpi suggested that the progression of G_1 phase should be

blocked during the later stage of infection. The expression of cyclin E, p-CDK2, and Cdc25A in infected cells also decreased at 15 hpi (Fig. 2B), suggesting that the G_1/S transition should also be blocked. The suppressed expression of these proteins at 15 hpi was consistent with the increased proportion of SIN-infected HeLa cells in G_1 phase at 15 hpi observed by FACS analysis. The suppression of p21 expression in infected cells was observed by 15 hpi, and might be caused by decreased p53 expression (Fig. 2B). By 15 hpi, the expression of cyclin A, which regulates the progression of S phase, had decreased in infected cells (Fig. 2C), suggesting that cells in S phase might be arrested during the later stage of infection.

To examine the function and time course of viral proliferation, we analyzed the expression of the capsid protein and two apoptotic indicators: cleaved caspase-3 and PARP fragment. The capsid protein was detected at 7 hpi (Fig. 3), indicating that SIN-induced promotion to S phase and the accumulation of cells in S phase occurred before structural proteins were expressed. Protein bands representing cleaved caspase-3 (19 kDa) and cleaved PARP fragment (89 kDa) were observed at 15 hpi (Fig. 3), indicating that apoptosis was induced at 15 hpi. The observation that apoptosis occurred at 15 hpi excluded the effect of SIN-induced apoptosis on the expression of cell cycle regulators during the early stage of infection and explained the reduced expression of cell cycle regulators at 15 hpi.

Viral replication and cell cycle phases in HeLa-Fucci and Vero-Fucci cells

FACS analysis and the effect of SIN infection on key cell cycle regulators demonstrated that HeLa cells were promoted into S phase and temporally arrested in

S phase during the early stage of infection, but Vero cells were not. The differences in the cell cycle progression of HeLa and Vero cells after SIN infection might reflect differences between cancer cells and non-cancerous cells regarding the status of the cell cycle. Such differences might cause variations in viral replication depending on cell cycle phase. To test this hypothesis, we simultaneously monitored SIN replication and a cell cycle indicator, Fucci, in HeLa and Vero cells.

We established HeLa-Fucci and Vero-Fucci cell lines by introducing pFucci-G_1 orange and pFucci-S/G_2/M Green-hyg successively into Vero and HeLa cells. In both cell lines, Fucci effectively labeled individual nuclei in G_1 phase as orange and those in S/G_2/M phases as green (Sakaue-Sawano et al., 2008). To label viral replication, HeLa-Fucci and Vero-Fucci were infected with TR339-BFP-2A, which contains the BFP gene between capsid and E3, and co-expresses BFP with viral structural proteins. After viral infection with TR339-BFP-2A, HeLa-Fucci and Vero-Fucci cells were imaged using a computer-assisted fluorescence microscope (Olympus, FV10i). Images were recorded every 30 min until most cells exhibited apoptosis.

The serially collected images of 217 infected HeLa-Fucci and 190 infected Vero-Fucci cells were traced and analyzed regarding cell cycle phases, the timing of the appearance of BFP fluorescence, and the time interval between BFP appearance and apoptosis. As shown in Table 1, the proportions of infected HeLa cells in G_1 and S/G_2/M phase at 2 hpi were 41% and 59%, respectively; these were equal with the proportions of total cells in G_1 (40%) and S/G_2/M phase (60%), respectively. The proportions of infected Vero cells in G_1 (57%) and S/G_2/M phases (43%) also

exhibited no obvious difference from the proportions of total cells in G_1 (51%) and $S/G_2/M$ phase (49%), respectively. These results suggested that HeLa-Fucci and Vero-Fucci cells in G_1 and $S/G_2/M$ phase are equally susceptible to SIN infection.

The proportions of BFP-expressing cells in respective cell cycle phases were as follows: HeLa-Fucci, 52% in G_1 and 48% in $S/G_2/M$; Vero-Fucci, 51% in G_1 and 49% in $S/G_2/M$. When the BFP-expressing cells were traced back to 2 hpi, the respective proportions of clones in cell cycle phases G_1 and $S/G_2/M$ were 41% and 59% for HeLa-Fucci and 47% and 53% for Vero-Fucci cells. Almost all cells underwent apoptosis during the same cell cycle phase at which BFP was expressed.

Cells infected during G_1 phase expressed BFP during G_1 or S/G_2 phase, and cells infected during S/G_2 phase expressed BFP during S/G_2 or after exiting M phase (Fig. 4A-D). The mean interval between adsorption and BFP expression in cells infected during G_1 was 9.3 h for HeLa cells and 8.9 h for Vero cells. The corresponding intervals were significantly longer for HeLa-Fucci and Vero-Fucci cells infected during $S/G_2/M$ (10.4 h and 10.2 h, respectively, Mann-Whitney U-test; $P < 0.05$) (Table 2). Apoptosis was always observed a few hours after the appearance of BFP (Table 2). The mean intervals between BFP appearance and apoptosis differed between cell lines (HeLa-Fucci: 3.8 hours; Vero-Fucci: 4.7 hours), but did not differ significantly between cells infected during G_1 phase and those infected during $S/G_2/M$ phase (Table 2). During the interval between BFP appearance and apoptosis, the color of Fucci changed only in a few cells that expressed BFP during M phase, indicating that most cells underwent cell cycle arrest once the virus started to replicate.

Sixty-nine percent of HeLa-Fucci cells infected with SIN during G_1 expressed BFP after entering S/G_2; in contrast, 31% of cells infected during G_1 phase expressed BFP during G_1 phase (Fig 5A). The preference for viral replication during S/G_2 phase in HeLa-Fucci cells was consistent with the promotion of the G_1/S phase transition by infection. Fewer Vero-Fucci cells infected during G_1 (52%) than HeLa-Fucci cells infected during G_1 expressed BFP during S/G_2 (chi-square test; $P < 0.05$) (Fig. 5B). Quite a few cells expressed BFP during M phase in both HeLa-Fucci and Vero-Fucci cells. The mean intervals between adsorption and BFP expression were significantly longer for cells that were infected during S/G_2 phase and progressed through M phase than for cells that did not progress through M phase (Mann-Whitney U-test; $P < 0.05$), suggesting that viral proliferation might be suspended during M phase.

SIN infection affects p53 expression differently in Vero cells, human fibroblasts, and HSC-4 cells

Generally, SIN infection causes cytopathic effects and apoptosis in mammalian cells (Frolov and Schlesinger, 1994). However, in some cell lines (e.g., HSC-4 cells), SIN can grow to a high titer with low cytopathogenicity (Saito et al., 2009b). In our results, the down-regulation of p53 and viral capsid expression were simultaneously observed in SIN-infected HeLa cells. Because p53 is an important regulator of apoptosis, we hypothesized that p53 might play an important role in the resistance of cancer cells (e.g., HSC-4 cells) to SIN-induced apoptosis. To test this hypothesis, we examined the effect of SIN infection on the expression of p53 and capsid protein in Vero cells, human fibroblasts, and HSC-4 cells.

In SIN-infected Vero cells, p53 levels decreased significantly at 4 hpi, followed by capsid protein expression at 7 hpi (Fig. 6A). In human fibroblasts, p53 expression decreased strikingly as the capsid protein was expressed at 15 hpi (Fig. 6B). In contrast, we observed a remarkable increase of p53 in HSC-4 cells (which harbor a mutant p53) as the capsid protein was expressed (Fig. 6C). Because p53 is a dominant-negative mutant in HSC-4 cells (Ichwan et al., 2006), the different response of p53 to SIN infection in HSC-4 cells may be attributable to the integrity of p53 protein. In addition, the resistance of HSC-4 cells to the oncolytic activity of SIN suggested a significant role for p53 in SIN-induced cytotoxicity.

Discussion

Both DNA and RNA viruses can alter the cell cycle to create a cellular environment that favors efficient replication (Reviewed by Emmett et al., 2005). In the present study, we observed that SIN infection altered the cell cycle progression in HeLa and Vero cells; however, these cell lines' responses to SIN infection differed during the early stage of infection. SIN infection caused HeLa cells to accumulate in S phase, with the proportion of cells in G_1 and G_2/M phases decreasing by 4 hpi. Consistently, SIN infection of HeLa cells affected the expression of CDK4 and CDK6 (G_1 phase regulators), cyclin E and p21 (G_1/S transition regulators), cyclin A (an S phase regulator), and cyclin B (a G_2/M transition regulator). Changes in the expression of cell cycle regulators during the early stage of SIN infection were considered to contribute to the promotion of the G_1/S transition and cell cycle retardation in S phase.

Using HeLa-Fucci cells infected with TR339-BFP-2A, we traced individual cells from infection to apoptosis. We confirmed that SIN, which infected HeLa cells but not Vero cells during G_1, preferred to proliferate during S/G_2, and the average length of time for viral replication was shorter in cells infected during G_1 than in cells infected during S/G_2/M phase. Because cells that expressed BFP during M phase were rare in Fucci expression experiments, viral proliferation appeared to be suspended during M phase. The suspension of viral proliferation in M phase might explain why the cells that were infected during S/G_2 and progressed through M took longer to express BFP.

A number of proteins involved in cell cycle control, including CDK2, p53, and p21, are distributed in the nucleolus, and their residence is dependent on cell cycle progression (Andersen et al., 2005). RNA viruses can hijack the nucleolus to usurp host cell functions and recruit nucleolar proteins to facilitate viral replication (reviewed by Hiscox, 2007). The alphavirus capsid protein and non-structural protein nsp2 have been shown to localize to the nucleoli of infected cells (Michel et al., 1990; Rikkonen et al., 1992). It remains to be determined whether these viral proteins located in the nucleolus affect the expression of cell cycle regulators, such as CDK4, CDK6, cyclin E, p21, and cyclin A.

Given that 80-90% of cellular RNA and protein synthesis is inhibited a few hours after infection by SIN (Gorchakov et al., 2005), it is noteworthy if the inhibition of RNA and protein synthesis is able to affect the expression of cell cycle regulators and cell cycle progression. In this study, after HeLa cells were infected with SIN, the expression of most cell cycle regulators exhibited no decrease at 7 hpi, but had decreased or disappeared by 15 hpi. Cell-cycle analyses between 7 and 15 hpi indicated that cell cycle progression still took place in infected HeLa cells. In experiments using Fucci-expressing cells, more than one-half of infected HeLa-Fucci and Vero-Fucci cells expressed BFP in cell cycle phases other than the phases during which infection occurred.

p53 is a key regulator that targets more than 150 genes associated with the regulation of cell cycle arrest, apoptosis, and DNA repair (El-Deiry, 1998; Amundson et al., 1998). As p53 is involved in antiviral innate immunity (it transactivates several

interferon-inducible genes) (Rivas et al., 2010), targeting and regulating p53 may be a strategy for viral infection and replication (Sato et al., 2009; Querido et al., 2001; Bhowmick et al., 2013; Sato and Tsurumi, 2013). During the later stage of SIN infection, when capsid proteins were produced, p53 expression was down-regulated in both HeLa and Vero cells, as well as human fibroblasts, but up-regulated in HSC-4 cells. The p53 protein in HeLa cells, human fibroblasts, and Vero cells is wild-type p53, while the p53 in HSC-4 cells is a dominant-negative mutant that effectively suppresses the function of p73 in apoptosis (Bergamaschi et al., 2003; Ichwan et al., 2006). The unresolved mechanism underlying the up-regulation of mutant p53 in SIN-infected HSC-4 cells might provide a clue to understanding the interaction between SIN infection and p53.

In conclusion, SIN infection can affect the expression of cell cycle regulators and drive cancer cells to accumulate in S phase. Affecting p53 expression during the later stage of viral infection might also be a strategy to achieve the efficient replication of SIN.

References

al-Saleh, W., Delvenne, P., van den Brule, F.A., Menard, S., Boniver, J., Castronovo, V., 1997. Expression of the 67 KD laminin receptor in human cervical preneoplastic and neoplastic squamous epithelial lesions: an immunohistochemical study. J. Pathol. 181 (3), 287-293.

Amundson, S.A., Myers T.G., Fornace, A.J. Jr., 1998. Roles for p53 in growth arrest and apoptosis: putting on the brakes after genotoxic stress. Oncogene 17 (25), 3287-3300.

Andersen, J.S., Lam, Y.W., Leung, A.K., Ong, S.E., Lyon, C.E., Lamond, A.I., Mann, M., 2005. Nucleolar proteome dynamics. Nature 433 (7021), 77-83.

Bergamaschi, D., Gasco, M., Hiller, L., Sullivan, A., Syed, N., Trigiante, G. et al., 2003. p53 polymorphism influences response in cancer chemotherapy via modulation of p73-dependent apoptosis. Cancer Cell 3 (4), 387-402.

Bhowmick, R., Halder, U.C., Chattopadhyay, S., Nayak, M.K., Chawla-Sarkar M., 2013. Rotavirus-encoded nonstructural protein 1 modulates cellular apoptotic machinery by targeting tumor suppressor protein p53. J. Virol. 87 (12), 6840-6850.

Chen, J., Kackson P.K., Kirschner, M.W., Dutta, A., 1995. Separate domains of p21 involved in the inhibition of Cdk kinase and PCNA. Nature 374 (6520), 386-388.

Demidova, A.R., Aau, M.Y., Zhuang, L., Yu, Q., 2009. Dual regulation of Cdc25A by Chk1 and p53-ATF3 in DNA replication checkpoint control. J. Biol. Chem. 284 (7), 4132-4139.

Dunphy, W.G., 1994. The decision to enter mitosis. Trends Cell Biol. 4 (6), 202-207.

El-Deiry, W.S., 1998. Regulation of p53 downstream genes. Semin Cancer Biol. 8 (5), 345-357.

Frolov, I., Schlesinger, S., 1994. Comparison of the effects of Sindbis virus and Sindbis virus replicons on host cell protein synthesis and cytopathogenicity in BHK cells. J. Virol. 68 (3), 1721-1727.

Emmett, S.R., Dove, B., Mahoney, L., Wurm, T., Hiscox, J.A., 2005. The cell cycle and virus infection. Methods Mol. Biol. 296, 197-218.

Goubin, F., Ducommun, B., 1995. Identification of binding domains on p21Cip1 cyclin-dependent kinase inhibitor. Oncogene 10 (12), 2281-2287.

Gorchakov, R., Frolova, E., Frolov, I., 2005. Inhibition of transcription and translation in Sindbis virus-infected cells. J. Virol. 79 (15), 9397-9409.

Griffin, D.E., 2001. Alphaviruses, in: Knipe D.M, Howley, P.M. (Eds.), Fields virology, ed. 4. Lippincott Williams and Wilkins, Philadelphia, pp. 917-962.

Gu, Y., Rosenblatt, J., Morgan, D.O., 1992. Cell cycle regulation of CDK2 activity by phosphorylation of Thr160 and Tyr15. EMBO J. 11 (11), 3995-4005.

Hiscox, J.A., 2007. RNA viruses: hijacking the dynamic nucleolus. Nat. Rev. Microbiol 5 (2), 119-127.

Hu, J., Cai, X.F., Yan, G., 2009. Alphavirus M1 induces apoptosis of malignant glioma cells via downregulation and nucleolar translocation of p21WAF1/CIP1 protein. Cell cycle 8 (20), 3328-3339.

Ichwan, S.J., Yamada, S., Sumrejkanchanakij, P., Ibrahim-Auerkari, E., Eto, K., Ikeda, M.A., 2006. Defect in serine 46 phosphorylation of p53 contributes to acquisition of p53 resistance in oral squamous cell carcinoma cells. Oncogene 25 (8), 1216-1224.

Jan, J.T., Griffin, D.E., 1999. Induction of apoptosis by Sindbis virus occurs at cell entry and does not require virus replication. J. Virol. 73 (12), 10296-10302.

Lin, G.Y., Lamb, R.A., 2000. The paramyxovirus simian virus 5 V protein slows progression of the cell cycle. J. Virol. 74 (19), 9152-9166.

Lukas, J., Herzinger, T., Hansen, K., Moroni, M.C., Resnitzky, D., Helin, K., Reed, S.I., Bartek, J., 1997. Cyclin E-induced S phase without activation of the pRb/E2F pathway. Genes Dev. 11 (11), 1479-1492.

Michel, M.R., Elgizoli, M., Dai, Y., Jakob, R., Koblet, H., Arrigo, A.P., 1990. Karyophilic properties of Semliki Forest virus nucleocapsid protein. J. Virol. 64 (10), 5123-5131.

Moriishi, K., Koura, M., Matsuura, Y., 2002. Induction of Bad-mediated apoptosis by Sindbis virus infection: involvement of pro-survival members of the Bcl-2 family. Virology 292 (2), 258-271.

Naniche, D., Reed, S.I., Oldstone, M.B., 1999. Cell cycle arrest during measles virus infection: a G_0-like block leads to suppression of retinoblastoma protein expression. J. Virol. 73 (3) 1894-1901.

Ohtsubo, M., Theodoras, A.M., Schumacher, J., Roberts, J.M., Pagano, M., 1995. Human cyclin E, a nuclear protein essential for the G_1-to-S phase transition. Mol. Cell. Biol. 15 (5), 2612-2614.

Op De Beeck, A., Caille-Fauquet, P., 1997. Viruses and the cell cycle. Prog. Cell cycle Res. 3, 1-19.

Pestell, R.G., Albanese, C., Reutens, A.T., Segall, J.E., Lee, R.J., Arnold, A., 1999. The cyclins and cyclin-dependent kinase inhibitors in hormonal regulation of proliferation and differentiation. Endocr. Rev. 20 (4), 501-534.

Querido, E., Blanchette, P., Yan, Q., Kamura, T., Morrison, M., Boivin, D., Kaelin, W. G., Conaway, R.C., Conaway, J.W., Branton, P.E., 2001. Degradation of p53 by adenovirus E4orf6 and E1B55K proteins occurs via a novel mechanism involving a Cullin-containing complex. Genes Dev. 15 (23), 3104-3117.

Resnitzky, D., Gossen, M., Bujard, H., Reed S.I., 1994. Acceleration of the G_1/S phase transition by expression of cyclins D1 and E with an inducible system. Mol. Cell. Biol. 14 (3), 1669-1679.

Rikkonen, M., Peränen, J., Kääriäinen, L., 1992. Nuclear and nucleolar targeting signals of Semliki Forest virus nonstructural protein nsP2. Virology 189 (2), 462-473.

Rivas C., Aaronson S.A., Munoz-Fontela, C., 2010. Dual Role of p53 in innate antiviral immunity. Viruses 2 (1), 298-313.

Saito, K., Shirasawa, H., Isegawa, N., Shiiba, M., Uzawa, K., Tanzawa, H., 2009a. Oncolytic virotherapy for oral squamous cell carcinoma using replication-competent viruses. Oral Oncol. 45 (12), 1021-1027.

Saito, K., Uzawa, K., Kasamatsu, A., Shinozuka, K., Sakuma, K., Yamatoji, M., Shiiba, M., Shino, Y., Shirasawa, H., Tanzawa, H., 2009b. Oncolytic activity of Sindbis virus in human oral squamous carcinoma cells. Br. J. Cancer 101 (4), 684-690.

Sakaue-Sawano, A., Kurokawa, H., Morimura, T., Hanyu, A., Hama, H., Osawa, H., Kashiwagi, S., Fukami, K., Miyata, T., Miyoshi, H., Imamura, T., Ogawa, M., Masai, H., Miyawaki, A., 2008. Visualizing spatiotemporal dynamics of multicellular cell cycle progression. Cell 132 (3), 487-498.

Sato, Y., Kamura, T., Shirata, N., Murata, T., Kudoh, A., Iwahori, S., Nakayama, S., Isomura, H., Nishiyama, Y., Tsurumi, T., 2009. Degradation of phosphorylated p53 by viral protein-ECS E3 ligase complex. PLoS Pathog. 5 (7), e1000530.

Sato, Y., Tsurumi, T., 2013. Genome guardian p53 and viral infections. Rev. Med. Virol. 23 (4), 213-220.

Shen, T., Huang, S., 2012. The role of Cdc25A in the regulation of cell proliferation and apoptosis. Anticancer Agents Med. Chem. 12 (6), 631-639.

Sherr, C. J., 1996. Cancer cell cycle. Science, 274 (5293), 1672-1677.

Thomas, J.M., Klimstra, W.B., Ryman, K.D., Heidner, H.W., 2003. Sindbis virus vectors designed to express a foreign protein as a cleavable component of the viral structural polyprotein. J. Virol. 77 (10), 5598-5606.

Tseng, J.C., Daniels, G., Meruelo, D., 2009. Controlled propagation of replication-competent Sindbis viral vector using suicide gene strategy. Gene Ther. 16 (2), 291-296.

Tseng, J.C., Levin, B., Hirano, T., Yee, H., Pampeno, C., Meruelo, D., 2002. In vivo antitumor activity of Sindbis viral vectors. J. Natl. Cancer Inst. 94 (23), 1790-1802.

Tseng, J.C., Levin, B., Hurtado, A., Yee, H., Perez De Castro, I., Jimenez, M., Shamamian, P., Jin, R., Novick, R.P., Pellicer, A., Meruelo, D., 2004. Systemic tumor targeting and killing by Sindbis viral vectors. Nat. Biotechnol. 22 (1), 70-77.

Tseng, J.C., Zanzonico, P.B., Levin, B., Finn, R., Larson, S.M., Meruelo, D., 2006. Tumor-specific in vivo transfection with HSV-1 thymidine kinase gene using a Sindbis viral vector as a basis for prodrug ganciclovir activation and PET. J. Nucl. Med. 47 (7), 1136-1143.

Unno, Y., Shino, Y., Kondo, F., Igarashi, N., Wang, G., Shimura, R., Yamaguchi, T., Asano, T., Saisho, H., Sekiya, S., Shirasawa, H., 2005. Oncolytic viral therapy for cervical and ovarian cancer cells by Sindbis virus AR339 strain. Clin. Cancer Res. 11 (12), 4553-4560.

van den Brûle, F.A., Castronovo, V., Ménard, S., Giavazzi, R., Marzola, M., Belotti, D., Taraboletti, G., 1996. Expression of the 67 kD laminin receptor in human ovarian carcinomas as defined by a monoclonal antibody, MLuC5. Eur. J. Cancer 32 A (9), 1598-1602.

Wang, K.S., Kuhn, R.J., Strauss, E.G., Ou, S., Strauss, J.H., 1992. High-affinity laminin receptor is a receptor for Sindbis virus in mammalian cells. J. Virol. 66 (8), 4992-5001.

Woo, R.A., Poon, R.Y., 2003. Cyclin-dependent kinases and S phase control in mammalian cells. Cell cycle 2 (4), 316-324.

Yamanaka, R., 2004. Alphavirus vectors for cancer gene therapy. Int. J. Oncol. 24 (4), 919-923.

Zeng, Y., Forbes K.C., Wu, Z., Moreno, S., Moreno, S., Piwnica-Worms, H., Enoch, T., 1998. Replication checkpoint requires phosphorylation of the phosphatase Cdc25 by Cds1 or Chk1. Nature 395 (6701), 507-510.

Table 1. HeLa-Fucci and Vero-Fucci cells infected with TR339-BFP-2A

	Cell cycle phase					
	HeLa-Fucci			Vero-Fucci		
	G_1	$S/G_2/M$	total	G_1	$S/G_2/M$	total
Total including uninfected at 2 hpi (%)	37(40)	62(60)	99	86(51)	78(49)	64
Infected at 2 hpi (%)	89(41)	128(59)	217	109(57)	81(43)	190
Expressing BFP						
Number of cells (%)	148(52)	134(48)	282	122(51)	116(49)	238
Number of clones (%)	89(41)	128(59)	217	90(47)	100(53)	190
Apoptosis (%)	150(53)	133(47)	283	128(53)	113(47)	241

Table 2. Kinetics of the SIN replication in HeLa-Fucci and Vero-Fucci cells, and the cell cycle phases at infection.

h of interval	Cell cycle phase at infection					
	HeLa-Fucci infected during			Vero-Fucci infected during		
	G_1	$S/G_2/M$	Mean	G_0/G_1	$S/G_2/M$	Mean
FP expression (h)	9.3*	10.4*	10.0	8.9†	10.2†	9.6
	(±2.0)	(±2.7)	(±2.6)	(±3.1)	(±3.4)	(±3.3)
poptosis (h)	13.1**	14.3**	13.8	13.7††	14.7††	14.3
	(±2.4)	(±3.0)	(±2.9)	(±3.5)	(±3.3)	(±3.4)
between BFP expression and	3.8	3.9	3.8	4.9	4.5	4.7
apoptosis (h)	(±1.3)	(±1.4)	(±1.4)	(±1.7)	(±1.4)	(±1.5)

Standard deviations are in parentheses.

* $P < 0.0001$; ** $P < 0.005$; † $P < 0.005$; †† $P < 0.01$ (all according to the Mann-Whitney U-test).

Fig. 1

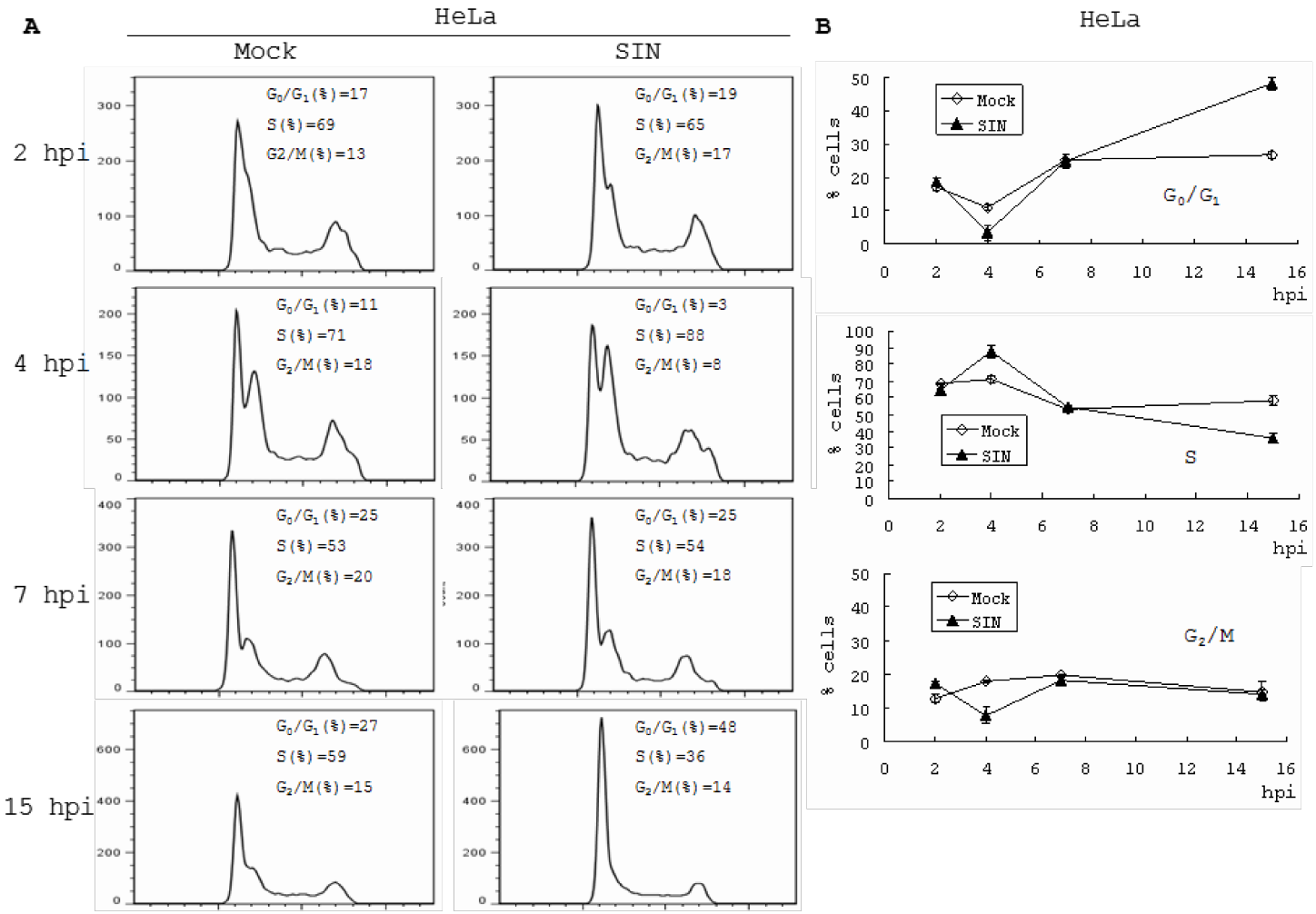
A
HeLa
Mock
SIN
2 hpi
4 hpi
7 hpi
15 hpi
G0/G1(%)=17
S(%)=69
G2/M(%)=13
G0/G1(%)=19
S(%)=65
G2/M(%)=17
G0/G1(%)=11
S(%)=71
G2/M(%)=18
G0/G1(%)=3
S(%)=88
G2/M(%)=8
G0/G1(%)=25
S(%)=53
G2/M(%)=20
G0/G1(%)=25
S(%)=54
G2/M(%)=18
G0/G1(%)=27
S(%)=59
G2/M(%)=15
G0/G1(%)=48
S(%)=36
G2/M(%)=14
B
HeLa
% cells
hpi
Mock
SIN
G0/G1
S
G2/M

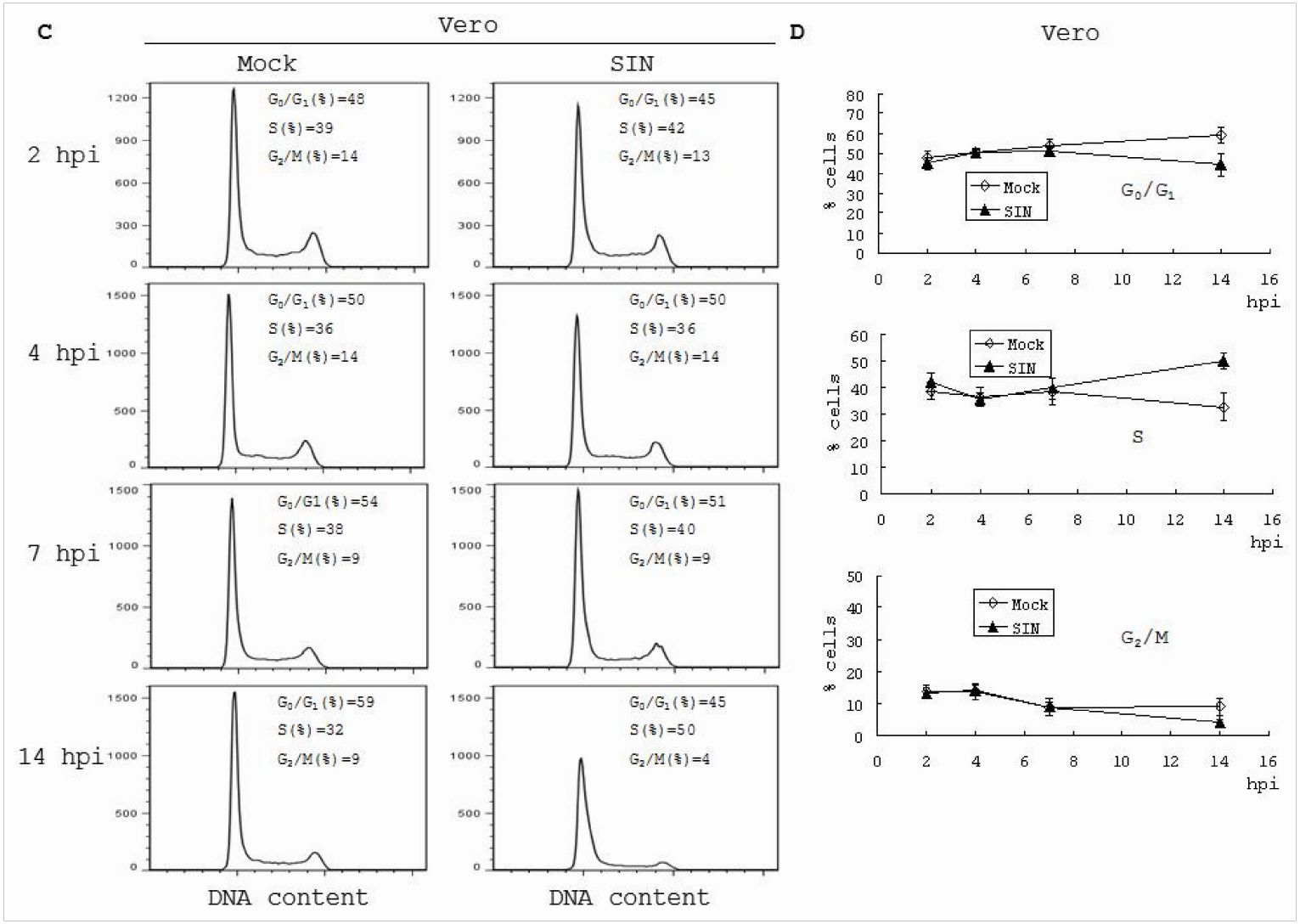
C
Vero
Mock
SIN
2 hpi
4 hpi
7 hpi
14 hpi
G0/G1(%)=48
S(%)=39
G2/M(%)=14
G0/G1(%)=45
S(%)=42
G2/M(%)=13
G0/G1(%)=50
S(%)=36
G2/M(%)=14
G0/G1(%)=50
S(%)=36
G2/M(%)=14
G0/G1(%)=54
S(%)=38
G2/M(%)=9
G0/G1(%)=51
S(%)=40
G2/M(%)=9
G0/G1(%)=59
S(%)=32
G2/M(%)=9
G0/G1(%)=45
S(%)=50
G2/M(%)=4
DNA content
DNA content
D
Vero
% cells
Mock
SIN
G0/G1
S
G2/M
hpi

Fig. 1. The effect of SIN infection on cell cycle progression. HeLa or Vero cells were infected with 1 MOI of SIN and subjected to FACS analysis at the indicated hour post-infection (hpi). (A) FACS analysis of mock-infected (Mock) and SIN-infected (SIN) HeLa cells at 2, 4, 7, and 15 hpi. Percentages of cells in G_0/G_1, S, and G_2/M are shown. (B) The time course of proportions of mock- and SIN-infected cells in G_0/G_1, S, and G_2/M phases. (C) FACS analysis of mock-infected (Mock) and SIN-infected (SIN) Vero cells at 2, 4, 7, and 14 hpi. Percentages of cells in G_0/G_1, S, and G_2/M are shown. (D) The time course of proportions of mock- and SIN-infected Vero cells in G_0/G_1, S, and G_2/M phases. Data presented are the mean of three independent experiments. Error bars indicate standard error.

Fig. 2

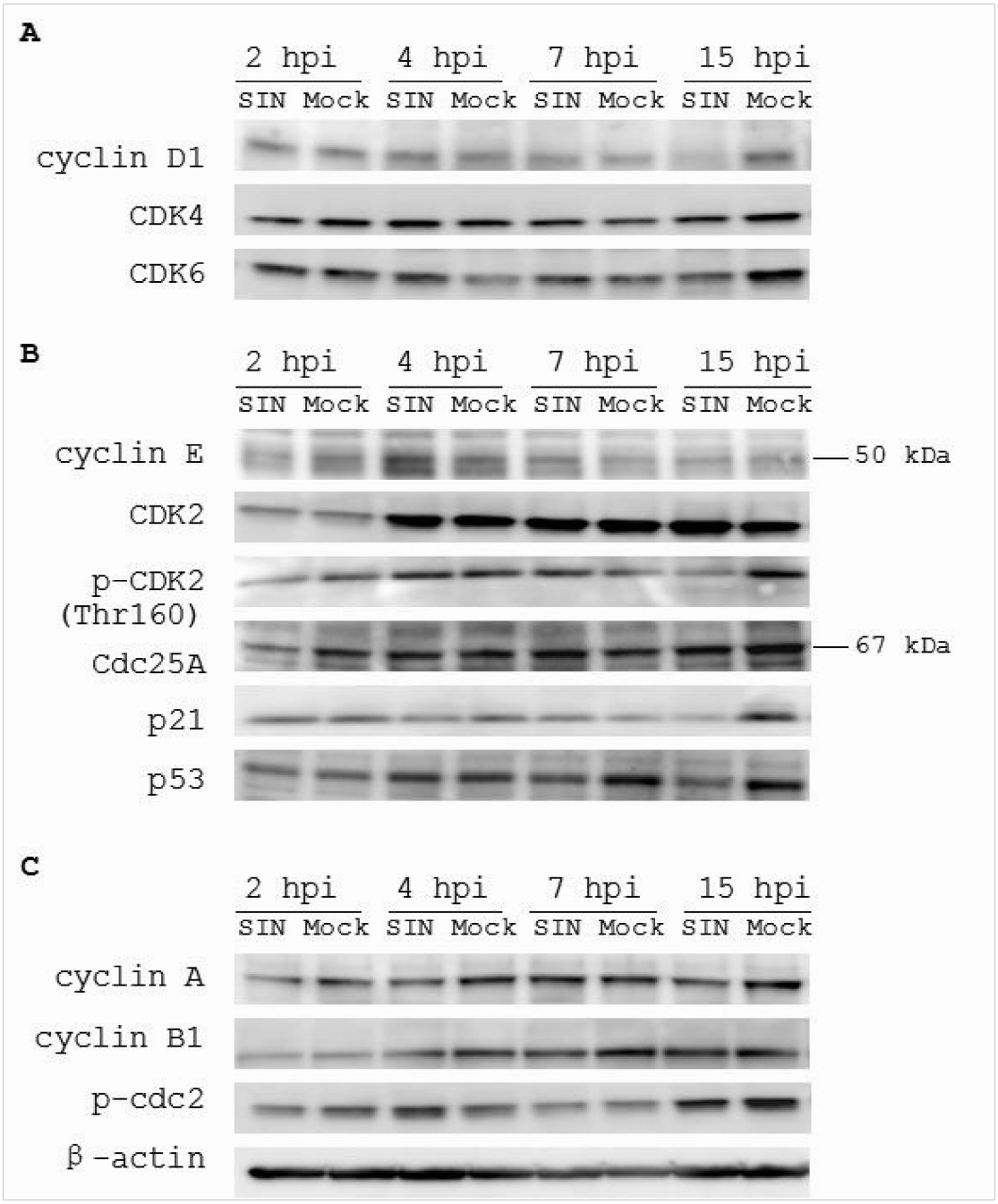
A
2 hpi
4 hpi
7 hpi
15 hpi
SIN Mock SIN Mock SIN Mock SIN Mock
cyclin D1
CDK4
CDK6
B
2 hpi
4 hpi
7 hpi
15 hpi
SIN Mock SIN Mock SIN Mock SIN Mock
cyclin E
50 kDa
CDK2
p-CDK2 (Thr160)
Cdc25A
67 kDa
p21
p53
C
2 hpi
4 hpi
7 hpi
15 hpi
SIN Mock SIN Mock SIN Mock SIN Mock
cyclin A
cyclin B1
p-cdc2
β-actin

Fig. 2. Western blots of mock- and SIN-infected HeLa cells assess the expression of cell cycle regulator proteins. Total protein from SIN-infected (SIN) and mock-infected (Mock) cells at 2, 4, 7, and 15 hours post-infection (hpi) were subjected to Western blotting. (A) Western blots of the G_1 phase regulators cyclin D1, CDK4, and CDK6. (B) Western blots of the G_1/S transition regulators cyclin E, CDK2, p-CDK2 (Thr160), Cdc25A, p21, and p53. The bars indicate the positions of cyclin E and Cdc25A. (C) Western blots of cyclin A, as well as G_2/M transition regulators cyclin B1 and p-cdc2. β-actin was an internal marker for equivalent protein loading.

Fig. 3

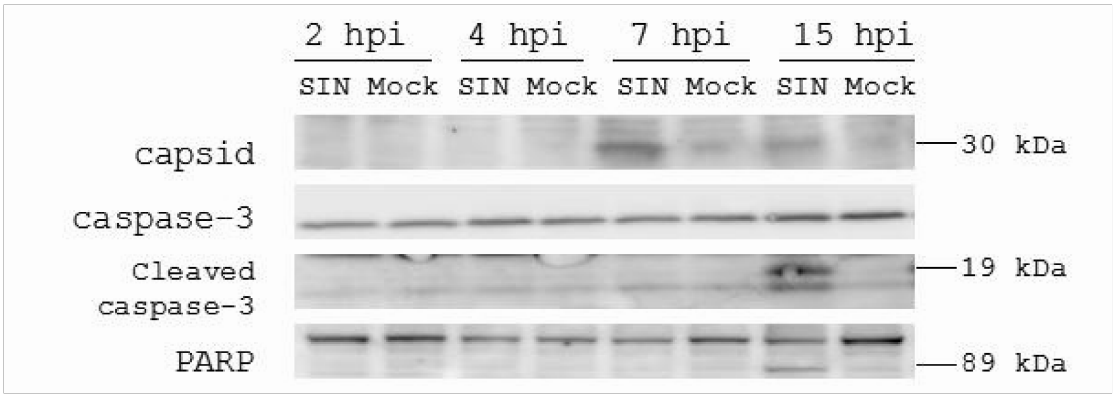
2 hpi
4 hpi
7 hpi
15 hpi
SIN Mock SIN Mock SIN Mock SIN Mock
capsid
caspase-3
Cleaved caspase-3
PARP
30 kDa
19 kDa
89 kDa

Fig.3. Western blots of mock- and SIN-infected HeLa cells assess the expression of capsid protein and pro-apoptotic proteins (caspase-3 and PARP). Total protein from SIN-infected (SIN) and mock-infected (Mock) cells at 2, 4, 7, and 15 hours post-infection (hpi) were subjected to Western blotting. The bars indicate the positions of capsid, cleaved caspase-3, and PARP bands.

Fig. 4

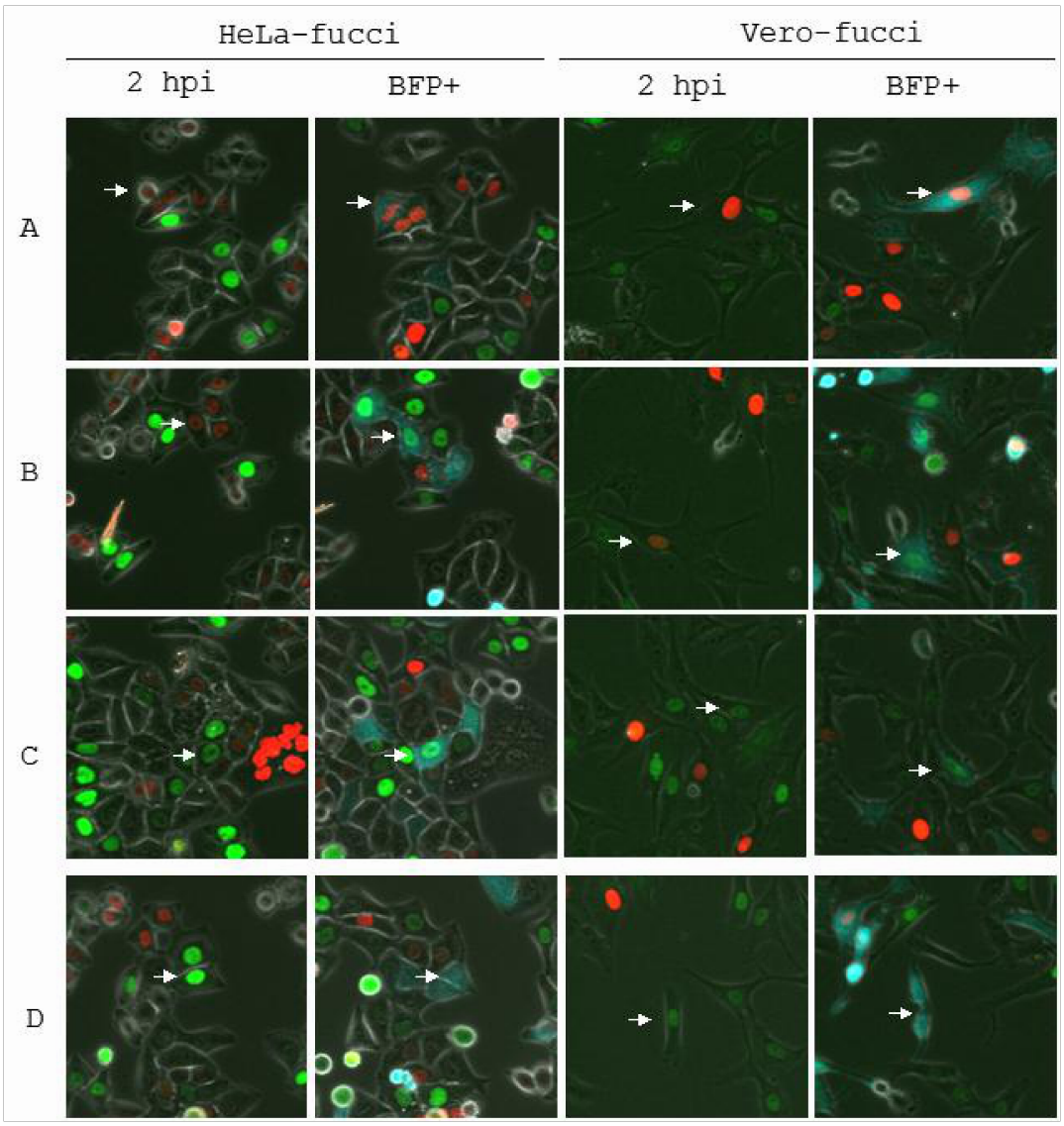

Fig. 4. The replication of BFP-expressing SIN, TR339-BFP-2A, in HeLa-Fucci and Vero-Fucci cells. Fucci labels nuclei orange during G_1 phase and green during $S/G_2/M$ phases. After infection with BFP-expressing SIN, TR339-BFP-2A, images of HeLa-Fucci and Vero-Fucci cells were obtained at 30-min intervals with a computer-assisted fluorescence microscope (Olympus, FV10i). Co-expression of blue fluorescent protein (BFP) with structural proteins from TR339-BFP-2A was observed in the cytoplasm. The lineage of each BFP-expressing cell was traced, and the cell cycle phase during which TR339-BFP-2A infection took place was determined. Arrows indicate cells that were infected during G_1 and expressed BFP during G_1 (A) or S/G_2 (B), cells that were infected during S/G_2 and expressed BFP during S/G_2 (C), or G_1 phase after cell division (D). The images shown were recorded at 2 hours post-infection (2 hpi) and at the time of BFP expression (BFP+).

Fig. 5

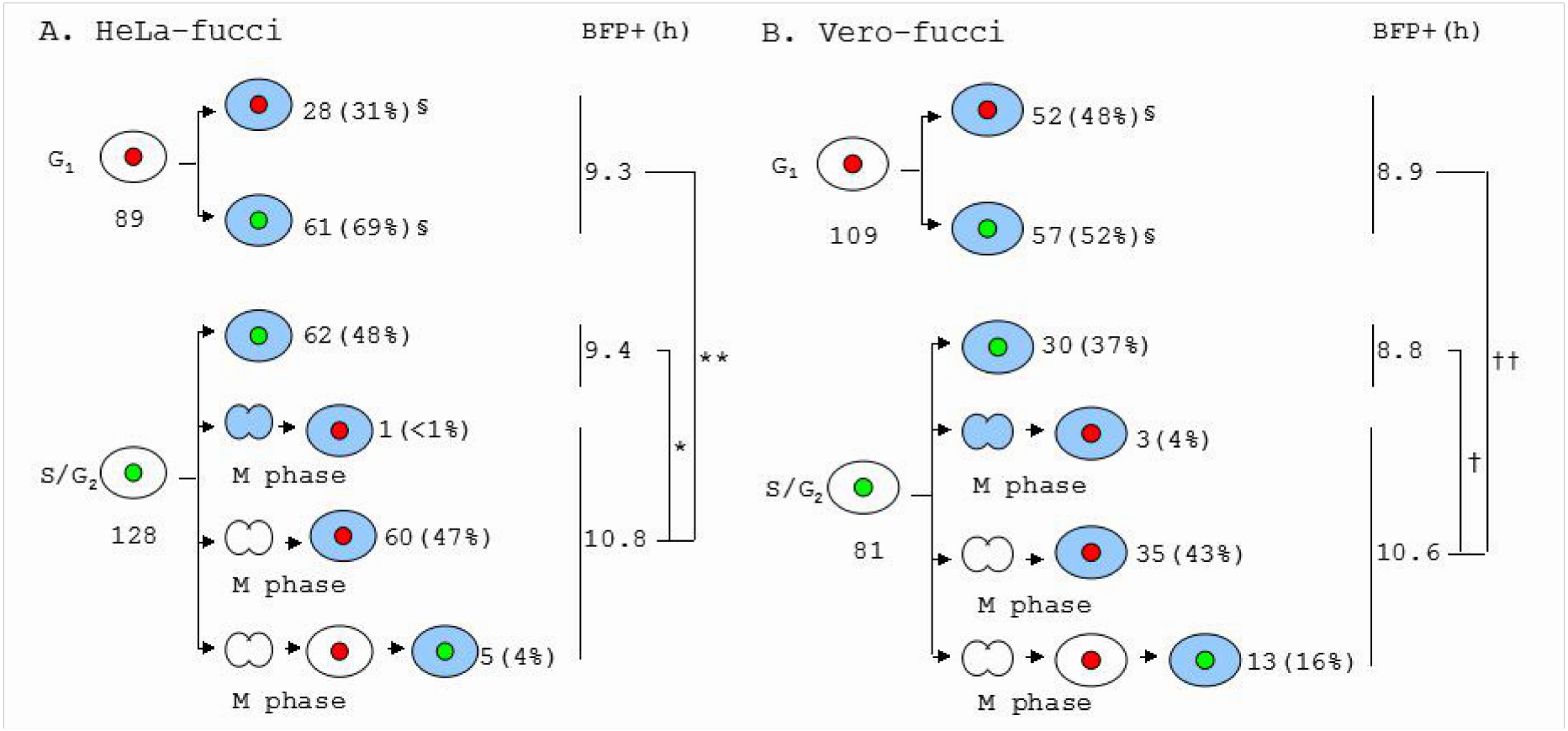
A. HeLa-fucci
BFP+(h)
G1
89
28 (31%)§
61 (69%)§
9.3
S/G2
128
62 (48%)
1 (<1%)
M phase
60 (47%)
M phase
5 (4%)
M phase
9.4
10.8
**
*
B. Vero-fucci
BFP+(h)
G1
109
52 (48%)§
57 (52%)§
8.9
S/G2
81
30 (37%)
3 (4%)
M phase
35 (43%)
M phase
13 (16%)
M phase
8.8
10.6
††
†

Fig. 5. Cell-cycle kinetics of HeLa-Fucci (A) and Vero-Fucci (B) cells infected with TR339-BFP-2A during G_1 and S/G_2 phase. Nuclei were labeled orange during G_1 and green during S/G_2. The lineage of each BFP-expressing cell was traced, and the cell cycle phase during which TR339-BFP-2A infection took place was determined (G_1 or S/G_2). The numbers of the traced cells are shown. The intervals between infection and BFP expression are shown at the right (BFP+). The distributions of BFP-expressing cells in G_1 and S/G_2 differed significantly between HeLa-Fucci and Vero-Fucci cells (§, $P < 0.05$, chi-square test). *$P < 0.005$; **$P < 0.0001$; †$P < 0.005$; ††$P < 0.00001$ (all according to the Mann-Whitney U-test).

Fig. 6

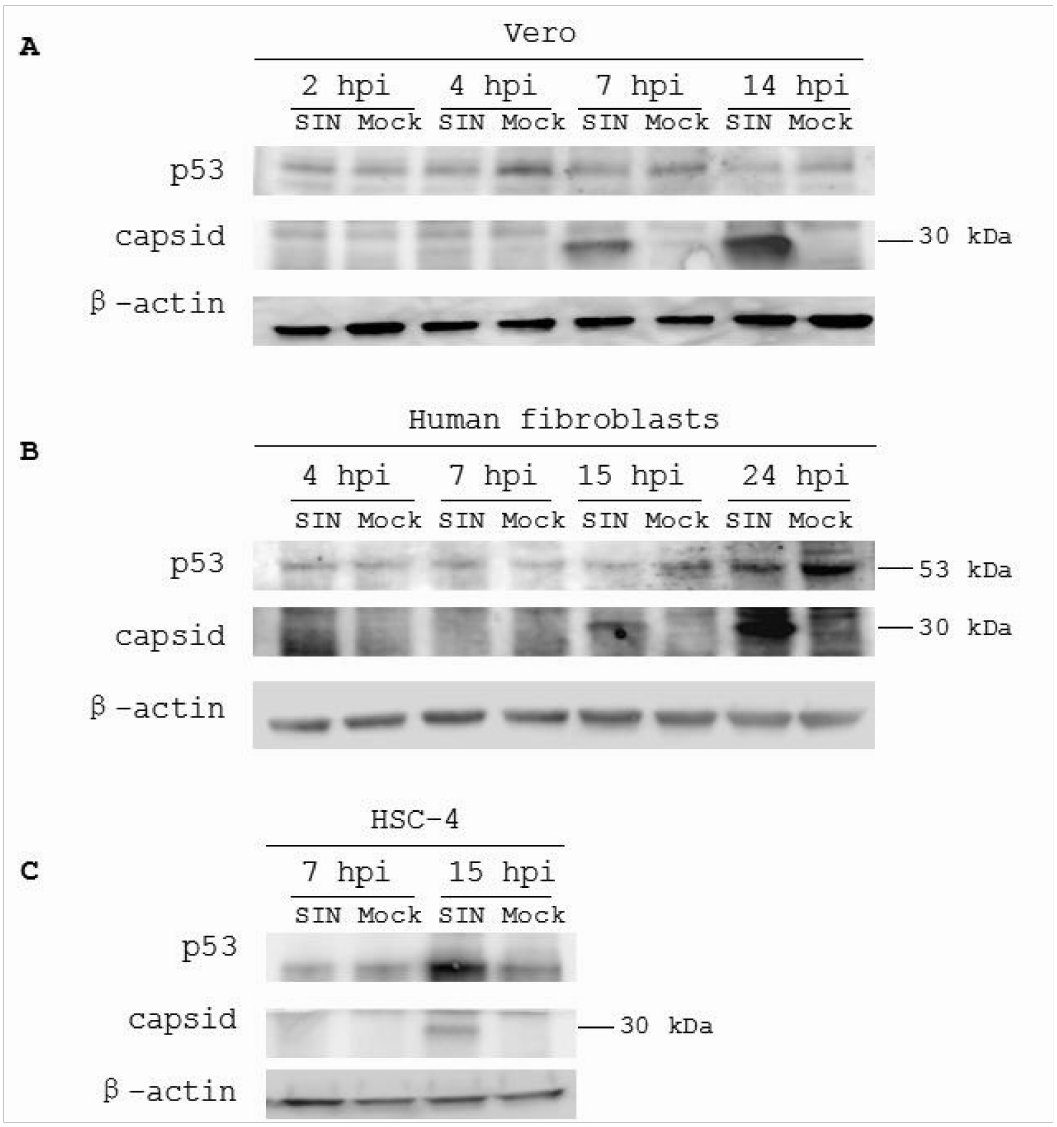
A
Vero
2 hpi
4 hpi
7 hpi
14 hpi
SIN Mock SIN Mock SIN Mock SIN Mock
p53
capsid
β-actin
30 kDa
B
Human fibroblasts
4 hpi
7 hpi
15 hpi
24 hpi
SIN Mock SIN Mock SIN Mock SIN Mock
p53
capsid
β-actin
53 kDa
30 kDa
C
HSC-4
7 hpi
15 hpi
SIN Mock SIN Mock
p53
capsid
β-actin
30 kDa

Fig. 6. Western blots of mock- and SIN-infected Vero cells (A), human fibroblasts (B), and HSC-4 cells (C) to assess the expression of p53 and the capsid proteins. Total protein was extracted from Vero, human fibroblast, and HSC-4 cells infected with SIN (SIN) or mock-infected (Mock) at the indicated time post-infection (hours post-infection, hpi) and were subjected to Western blotting with antibodies raised against p53, capsid protein, and β-actin. β-actin was an internal marker for equivalent protein loading. The bars indicate the positions of p53 and capsid.

Biochemical and Biophysical Research Communications Vol. 462 No 426-432
平成27年7月10日　公表済